Distribution, Metabolism, and Elimination of Phenobarbital in Rats: Physiologically Based Pharmacokinetic Model

J. M. ENGASSER* ˣ, F. SARHAN ‡, C. FALCOZ *, M. MINIER *, P. LETOURNEUR *, and G. SIEST ‡

Received February 15, 1980, from the **Laboratoire des Sciences du Génie Chimique, CNRS-ENSIC, 1, rue Grandville, 54042 Nancy Cedex, France*, and the ‡*Laboratoire de Biochimie Pharmacologique, Faculté de Pharmacie, 7, rue Albert Lebrun, 54001 Nancy, France.*
Accepted for publication March 26, 1981.

Abstract □ The distribution, metabolism, and elimination kinetics at two different doses of phenobarbital were examined in rats. After intravenous injection, phenobarbital distributed very rapidly to the liver and kidneys, less rapidly to the muscle and gut, and much more slowly to the brain. At the higher dose, a concentration rebound was observed 1 hr after injection. In addition, phenobarbital distributed unevenly in various organs as a result of a different extent of drug binding. A physiologically based model, including enterohepatic cycling and diffusion resistances between blood and tissue, is proposed for phenobarbital pharmacokinetics. It satisfactorily describes phenobarbital distribution in rats at the two doses and allows an evaluation of fundamental physicobiochemical parameters such as drug–tissue binding constants, blood–tissue transport coefficients, metabolism, and elimination rate constants.

Keyphrases □ Phenobarbital—physiologically based model for distribution, metabolism, and elimination kinetics in rats □ Models, pharmacokinetic—for phenobarbital distribution, metabolism, and elimination, rats □ Pharmacokinetics—model for phenobarbital distribution, metabolism, and elimination, rats

Physiologically based models are being used more frequently in pharmacokinetic studies (1, 2). Based on anatomical and physiological characteristics and on drug physicochemical parameters, these models greatly facilitate pharmacokinetic data interpretation and allow extrapolation outside the data range and to other species. Physiological models are of greatest interest for the determination of basic physicobiochemical parameters relating to drug disposition and action and for the rational design of drug posology. Their potential was recently illustrated for anticancer drugs (2) and for digoxin (3), thiopental (4, 5), and pesticides (6).

The present study, which examined the distribution, metabolism, and elimination of phenobarbital following intravenous injection in rats, proposes a physiologically based pharmacokinetic model for phenobarbital. The drug, known to have different pharmacological action (sedative, hypnotic, and antiepileptic) depending on its concentration level in the brain, is also a powerful inducer of hepatic metabolizing enzymes (7). A physiological model considering phenobarbital diffusion to the brain, metabolism in the liver, binding to proteins and tissues, renal elimination, and intestinal resorption following biliary excretion can satisfactorily describe phenobarbital distribution and fate in rats.

EXPERIMENTAL

Male Sprague–Dawley rats[1], 200–240 g, were injected intravenously with an isotonic sodium chloride solution of phenobarbital sodium[2]. Two doses, 30 and 50 mg/kg, were used. At different times after injection in the tail vein, the rats were decapitated, and blood and tissues were collected. After blood centrifugation at 9000 rpm, plasma was separated. Tissues and plasma were then stored at −14° until analysis.

Phenobarbital was extracted from plasma, urine, and bile using a one-step extraction procedure with chloroform; drug extraction from tissues and feces was performed with a previously described, two-step procedure with chloroform (8). Phenobarbital was then assayed in a gas chromatograph equipped with a nitrogen selective detector (9) to improve assay specificity and sensitivity. Analysis sensitivity is <1 μg of phenobarbital/sample.

For the evaluation of urinary excretion, rats were placed in metabolic cages. Urine, free from fecal contamination, was collected at timed intervals and then assayed for phenobarbital. The biliary excretion of phenobarbital was determined on bile duct-cannulated rats previously anesthetized with ether.

Drug binding to plasma proteins was measured with an equilibrium dialysis system[3]. When using 1-ml polytef[4] dialysis cells with cellulose membranes[5], binding equilibrium can be rapidly achieved. Experiments were performed with undiluted plasma adjusted to pH 7.35 by carbogen (5% carbon dioxide, 95% oxygen) bubbled on one side of the membrane and an isotonic phosphate buffer (pH 7.35), initially spiked with phenobarbital, on the other side. Phenobarbital binding to the membrane was <5%. A total plasma concentration of 10–110 μg/ml was investigated.

RESULTS

Figure 1 shows the measured distribution of phenobarbital in the blood, liver, brain, muscle, intestine, and kidneys at the two injected doses of 50 and 30 mg/kg. Each point represents the mean obtained for five rats, with a standard deviation between 15 and 20%. The following pharmacokinetic characteristics can be observed. First, while phenobarbital distributed very rapidly in the liver and kidneys, it entered more slowly in brain, muscle, and intestine, probably because of mass transport limitations. The slowness of drug diffusion was particularly pronounced in the brain where the maximum concentration was reached only after 1 hr at the two investigated doses.

Second, a concentration rebound was observed in blood and several organs, ~1 hr after drug injection, at least at the higher dose. This phenomenon may be the result of enterohepatic cycling[6]. A biliary excretion of unchanged phenobarbital (~110 μg in the 1st hr at the high dose) was indeed observed in bile duct-cannulated rats.

Third, during the elimination phase, the concentration remained at different levels in the various organs, with the liver presenting the highest phenobarbital affinity. This result suggests different binding extents by plasma proteins and tissues.

Further insight into the kinetics of the limiting processes is obtained by plotting the ratio of the drug concentration over the administered dose. As seen in Fig. 2 for the various tissues, the points corresponding to the two doses come close together, indicating that phenobarbital pharmacokinetics can be considered dose independent at the investigated concentrations. Consequently, in a first approximation, first-order transport, metabolism, and excretion processes, as well as linear phenobarbital binding to plasma proteins and tissues, may be assumed.

[1] Domaine des Oncins, Saint-Germain sur l'Arbresle, France.
[2] Merck.
[3] Dianorm apparatus, Diachema, Birmenstorf, Zurich, Switzerland.
[4] Teflon.
[5] Spectrapor 2, Spectrum Medical Industries, Los Angeles, Calif.
[6] J. Caldwell, J. E. Croft, and R. L. Smith, St. Mary's Hospital Medical School, London, England, to be published.

0022-3549/81/1100-1233$01.00/0

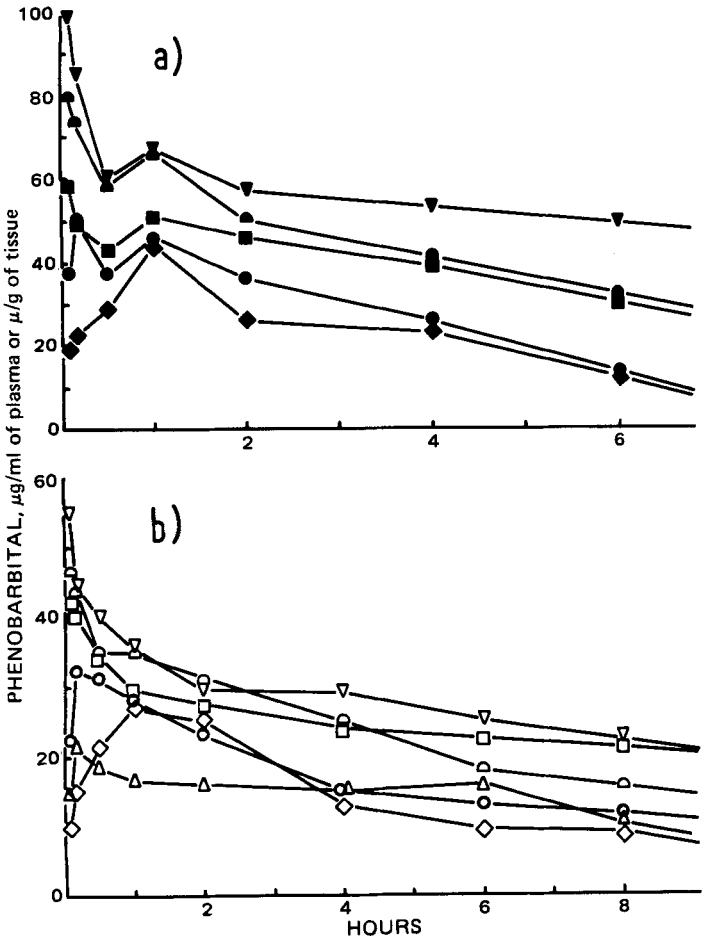

Figure 1—*Time evolution of phenobarbital distribution in rat tissues after intravenous injection of 50 (a) and 30 (b) mg/kg. Key (solid symbols for a and open symbols for b): ◓, ◔, plasma; ♦, ◇, brain; ▼, ▽, liver; ■, □, kidneys; and ●, ○, muscle; △, gut.*

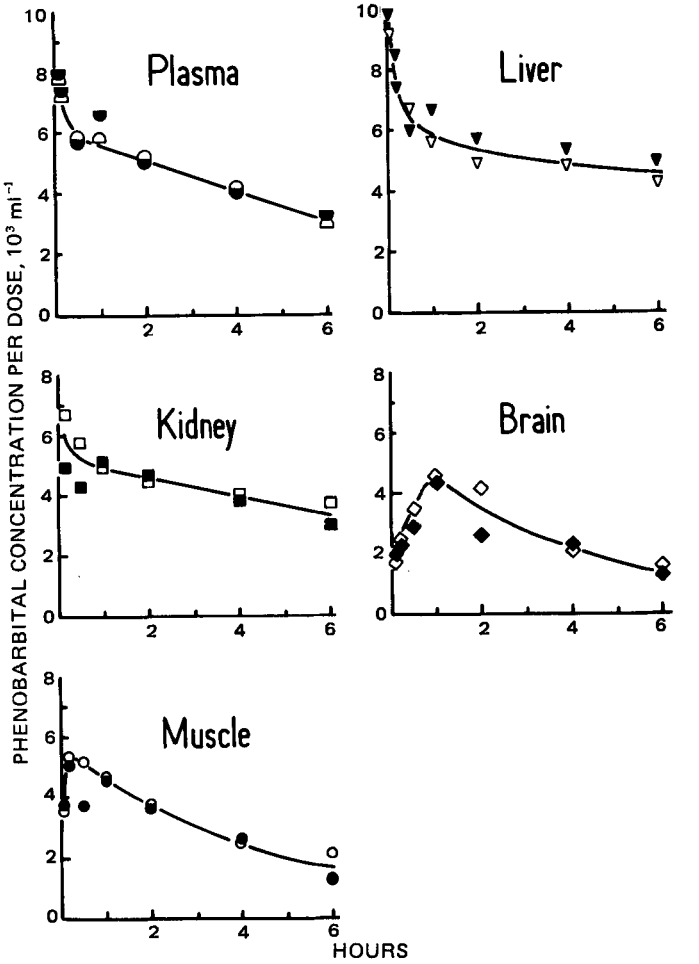

Figure 2—*Variation with time of the ratio of phenobarbital concentration over the administered dose in various rat tissues as calculated from Fig. 1 Key: solid symbols, 50 mg/kg; and open symbols, 30 mg/kg.*

The kinetics of urinary excretion were independently determined by simultaneously measuring the rate of urinary excretion and plotting the results as a function of drug plasma concentration. Figure 3 shows that the elimination rate was proportional to plasma concentration for concentrations of <30 μg/ml, with, however, the rate falling off at higher levels. During the first 24 hr, the total amount of excreted unchanged phenobarbital was ~10% of the administered dose.

THEORY

Flow-Sheet Diagram—In its basic structure, the model in Scheme I is similar to models previously proposed for other drugs (4, 10). It depicts the main organs (brain, liver, gut, kidneys, and muscles) represented by a physiological compartment and connected by the blood network. Moreover, each organ and tissue is subdivided into the flowing blood and the tissue region. Tissues not experimentally considered are lumped into an additional compartment, called "remaining distribution volume," analogous to the distribution volume concept introduced in classical pharmacokinetics.

In view of the previous experimental results, the model also takes into account the enterohepatic cycle. The progress of the biliary-secreted drug towards the gut is handled by a plug flow compartment with a given residence time. Since the intestinal resorption of phenobarbital is relatively fast, the excreted drug is assumed to be directly transferred to the gut tissue.

In addition, this model includes some diffusional limitations between the perfusing blood and the brain, muscle, and intestinal tissues. In other organs, drug membrane transport is fast enough to assume equilibrium between blood and tissue.

To account for drug elimination, the model also considers drug metabolism in the liver tissue and urinary excretion in the kidney.

Injection—To represent intravenous administration of the drug, the injection function $Dg(t)$ proposed by Bischoff and Dedrick (4) was used such that:

$$g(t) = \frac{30}{\theta}\left(\frac{t}{\theta}\right)^2\left(1 - \frac{t}{\theta}\right)^2 \qquad \text{(Eq. 1)}$$

where $g(t)$ is a normalized impulse function (minutes^{-1}), θ is the injection duration (minutes), and D is the total dose (micrograms).

Drug Binding to Plasma Proteins—The total blood concentration can be expressed as:

$$C^*_{Bl} = (1 - \text{HEM})\, C^*_P + \text{HEM}\, C^*_{BlC} \qquad \text{(Eq. 2)}$$

where:

C^*_{Bl} = total blood concentration (micrograms per milliliter)
C^*_P = total plasma concentration
C^*_{BlC} = total blood cell concentration.
HEM = hematocrit (dimensionless)

It was observed experimentally that for phenobarbital the total blood concentration is equal to the total plasma concentration, *i.e.*:

$$C^*_{Bl} = C^*_P = C^*_{BlC} \qquad \text{(Eq. 3)}$$

Blood may thus be assimilated to plasma.

In the plasma, it is necessary to distinguish between the free and bound drug concentration:

$$C^*_P = C_P + C'_P \qquad \text{(Eq. 4)}$$

where C_P is the free plasma concentration, and C'_P is the bound plasma concentration.

According to drug binding experiments, there is a linear relationship between plasma bound and free phenobarbital concentrations, *i.e.*:

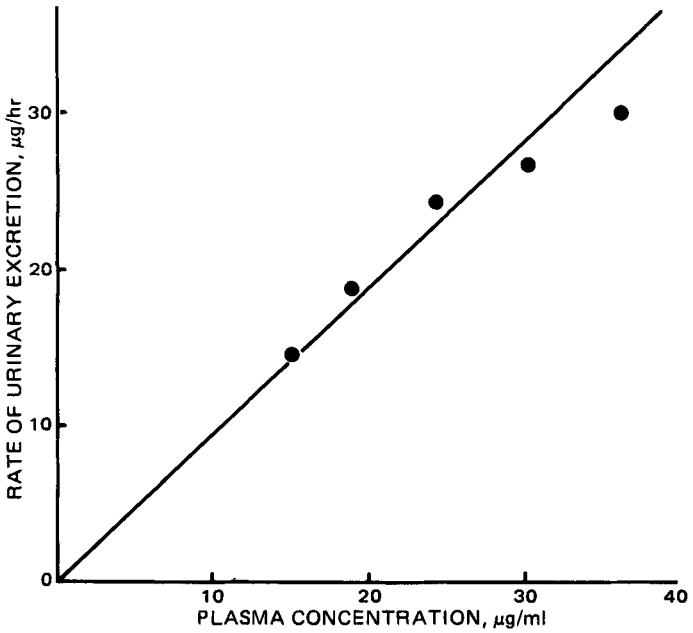

Figure 3—*Rate of urinary phenobarbital excretion as a function of plasma concentration after a 30-mg/kg iv dose. The rate was calculated from the quantity of phenobarbital excreted over 2 hr, and the corresponding plasma concentration is the one at the middle of the collection period. The urinary elimination rate constant was evaluated from the slope of the line drawn through the experimental points.*

$$C'_P = b_P C_P \qquad \text{(Eq. 5)}$$

where b_P represents the plasma binding constant. Accordingly, the total plasma concentration is simply related to the free concentration by:

$$C^*_P = (1 + b_P)C_p \qquad \text{(Eq. 6)}$$

Drug Binding to Tissues—As previously proposed (4), the total tissue concentration is expressed as:

$$C^*_T = f_T C_T + (1 - f_T)C'_T \qquad \text{(Eq. 7)}$$

where:

C^*_T = total tissue concentration
C_T = free tissue concentration
C'_T = bound tissue concentration
f_T = water fraction of tissue (dimensionless)

Preliminary binding experiments with diluted muscles, as well as other results (11) with rat lung and liver slices, suggest a linear relationship for phenobarbital tissue binding, *i.e.*:

$$C'_T = b_T C_T \qquad \text{(Eq. 8)}$$

where b_T is the binding constant of the tissue. Under these conditions:

$$C^*_T = [f_T + (1 - f_T)b_T]C_T \qquad \text{(Eq. 9)}$$

According to Eqs. 6 and 9, for blood and tissues the total concentration, C^*, is proportional to the free concentration, C:

$$C^* = \Phi C \qquad \text{(Eq. 10)}$$

where:

$$\Phi = f + (1 - f)b \qquad \text{(Eq. 11)}$$

The proportionality constant, Φ, represents the binding ability of blood and tissues (12).

Blood–Tissue Distribution—In organs where the transport of drug between blood and tissue is very fast, equal free concentrations in plasma and tissue were assumed, *i.e.*:

$$C_T = C_P \qquad \text{(Eq. 12)}$$

However, in brain, muscle, and gut, drug transport between blood and tissue may represent a limiting process. Under these conditions the transport rate is expressed as:

$$r_t = H(C_P - C_T) \qquad \text{(Eq. 13)}$$

where r_t is the drug transport rate from plasma to tissue (μg/min), and H is the drug transport coefficient or tissue permeability (ml/min).

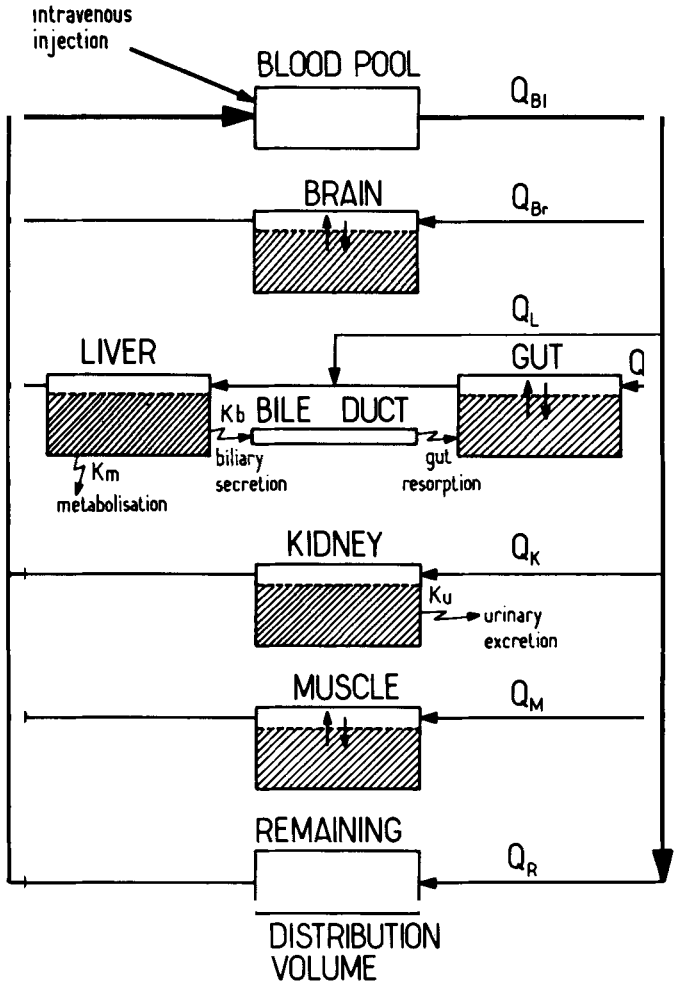

Scheme I—Physiological pharmacokinetic model for phenobarbital.

Drug Elimination Processes—Phenobarbital elimination by urinary excretion, hepatic metabolism, and biliary excretion is assumed to be a first-order process and thus is represented by:

$$r_e = KC_T \qquad \text{(Eq. 14)}$$

where:

r_e = elimination rate (μg/min)
K = elimination (excretion or metabolism) rate constant (ml/min)
C_T = free concentration in elimination tissue (μg/ml)

The total amount of drug, E (in micrograms), excreted in a given organ is equal to:

$$E = \int_0^t KC_T\,dt \qquad \text{(Eq. 15)}$$

where t is time (minutes).

Mass Balance Equations—The resulting mass balance equations for the various compartments are as follows (notation is given in the *Appendix*).

For blood:

$$V_{Bl}\Phi_{Bl}\frac{dC_{Bl}}{dt} = Dg(t) + \Phi_{Bl}\,[Q_{Br}C_{Br,Bl} + (Q_L + Q_G)C_{L,Bl} + Q_K C_{K,Bl} + Q_M C_{M,Bl} + Q_R C_R - Q_{Bl}C_{Bl}] \qquad \text{(Eq. 16a)}$$

where:

$$Q_R = Q_{Bl} - Q_{Br} - Q_L - Q_G - Q_K - Q_M \qquad \text{(Eq. 16b)}$$

Table I—Values of parameters for a Standard 200-g Male Rat [a]

Compartment	Physiological Parameters: Volume, ml Tissue	Volume, ml Blood[b]	Blood Flow, ml/min	Water Fraction[c] (f)	Pharmacokinetic Parameters: Binding Constant (b)	Binding Ability (Φ)	Transfer Coefficient, ml/min	Elimination Constant, ml/min
Blood		13	58(*)	—	1.1	2.1		
Brain	2	0.022	2	0.80	1.1	1.	0.15	
Gut	5.6	0.23	8.5	0.76	1.7	1.2	20	$K_b = 1$
Liver	6.7	0.7	1	0.75	6.7	2.4		$K_m = 0.4$
Kidneys	2.3	0.21	8.5	0.80	6.1	2.		$K_u = 0.04$
Muscle	93	0.4	10	0.78	3.6	1.6	50	
Remaining distribution volume		55	28[d]					

[a] References 3, 5, and 13–23. [b] Blood permitted to ooze from tissue (13). [3] From dog values (5). [d] Calculated from difference between total cardiac output (*) and the sum of the tissue blood flows.

For brain blood:

$$V_{Br,Bl}\Phi_{Bl}\frac{dC_{Br,Bl}}{dt} = Q_{Br}\Phi_{Bl}(C_{Bl} - C_{Br,Bl}) + H_{Br}(C_{Br,T} - C_{Br,Bl}) \quad \text{(Eq. 17a)}$$

For brain tissue:

$$V_{Br,T}\Phi_{Br}\frac{dC_{Br,T}}{dt} = H_{Br}(C_{Br,Bl} - C_{Br,T}) \quad \text{(Eq. 17b)}$$

For gut blood:

$$V_{G,Bl}\Phi_{Bl}\frac{dC_{G,Bl}}{dt} = Q_G\Phi_{Bl}(C_{Bl} - C_{G,Bl}) + H_G(C_{G,T} - C_{G,Bl}) \quad \text{(Eq. 18a)}$$

For gut tissue:

$$V_{G,T}\Phi_G\frac{dC_{G,T}}{dt} = H_G(C_{G,Bl} - C_{G,T}) + K_bC_{L,T}^{(t-T_{del})} \quad \text{(Eq. 18b)}$$

where $C_{L,T}^{(t-T_{del})}$ is the free tissular liver concentration at time $(t - T_{del})$.

For liver:

$$C_{L,Bl} = C_{L,T} = C_L \quad \text{(Eq. 19a)}$$

$$(V_{L,Bl}\Phi_{Bl} + V_{L,T}\Phi_L)\frac{dC_L}{dt} = \Phi_{Bl}[Q_GC_{G,Bl} + Q_LC_{Bl} - (Q_G + Q_L)C_L] - (K_m + K_b)C_L \quad \text{(Eq. 19b)}$$

For kidney:

$$C_{K,Bl} = C_{K,T} = C_K \quad \text{(Eq. 20a)}$$

$$(V_{K,Bl}\Phi_{Bl} + V_{K,T}\Phi_K)\frac{dC_K}{dt} = Q_K\Phi_{Bl}(C_{Bl} - C_K) - K_uC_K \quad \text{(Eq. 20b)}$$

For muscle blood:

$$V_{M,Bl}\Phi_{Bl}\frac{dC_{M,Bl}}{dt} = Q_M\Phi_{Bl}(C_{Bl} - C_{M,Bl}) + H_M(C_{M,T} - C_{M,Bl}) \quad \text{(Eq. 21a)}$$

For muscle tissue:

$$V_{M,T}\Phi_M\frac{dC_{M,T}}{dt} = H_M(C_{M,Bl} - C_{M,T}) \quad \text{(Eq. 21b)}$$

For the remaining distribution volume:

$$V_R\frac{dC_R}{dt} = Q_R(C_{Bl} - C_R) \quad \text{(Eq. 22)}$$

The resulting set of nonlinear differential equations is solved simultaneously with a fourth-order Runge–Kutta method on a digital computer.

Values of Parameters—The various anatomic and physiological parameters, blood flow rates, tissue volumes, and water fractions for a 200-g male rat are summarized in Table I. The remaining distribution volume was determined by fitting the theoretical curves to the experimental results.

For the intravenous drug injection, a value of 0.25 min for θ is representative of the experimental conditions.

The plasma binding constant b_P was experimentally determined as 1.1, which corresponds to a proportionality constant, Φp, of 2.1 between the total and free plasma concentration. The binding constants b_T for the tissues as defined in Eq. 8 were obtained by curve fitting. They were most precisely determined from the different drug levels in the elimination phase, as experimentally observed in Fig. 1. The resulting values of b_T and the tissue binding ability Φ_T, *i.e.*, the proportionality constant between total and free concentration, are shown in Table I.

The urinary elimination constant, K_u, defined in Eq. 20*b* as the proportionality constant between the rate of urinary elimination and the free tissue, *i.e.*, free plasma, concentration in the kidney can be simply evaluated from the slope of the line obtained on Fig. 3 as 0.04 ml/min.

The metabolism rate constant K_m, which, according to Eq. 14, relates the rate of metabolism to the free liver tissue concentration, was estimated by dividing the amount of drug metabolized, ~80% of the dose, during the first 24 hr by the area under the free plasmatic concentration *versus* time curve (assuming equal free plasma and free liver tissue concentration):

$$K_m = (1 + b_P)\frac{\int_0^{24} K_mC_L\,dt}{\int_0^{24} C_P\,dt} \quad \text{(Eq. 23)}$$

This evaluation procedure yields a value of 0.4 ml/min for K_m.

As previously suggested (12), the passage of the drug through the enterohepatic cycle was approximated in Eq. 18*b* by a delay time, T_{del}, which approximates the drug travel through the bile and down the small intestine before absorption in the gut tissue. This residence time, T_{del}, through the enterohepatic cycle was adjusted to 55 min to obtain a concentration rebound ~1 hr after drug injection. The magnitude of the biliary excretion constant, K_b, which directly determines the height of the concentration rebound, was chosen as 1 ml/min.

Finally, blood–tissue transfer coefficients in brain, muscle, and gut were determined by fitting the theoretical curves to the experimentally observed tissue concentrations during the distribution phase. The corresponding values are given in Table I.

DISCUSSION

The theoretical drug distribution curves in the various compartments obtained with the previously defined model are shown in Fig. 4. The two sets of curves corresponding to the two injected doses of 30 and 50 mg/kg were calculated with the same physiological and pharmacokinetic parameters (Table I).

Although in its present state the model does not perfectly describe the observed phenobarbital distribution, it appears satisfactory in many respects. It is the simplest possible model based on the animal anatomy and taking into account key physiological parameters such as protein and tissue binding, liver metabolism, renal excretion, bile excretion, intestinal reabsorption, and tissue diffusion. This model, which only entails simple first-order physical and chemical rate processes, can especially account for the slow drug penetration in the brain, for the concentration rebound 1 hr after injection, and for different tissue drug levels during the elimination phase. Moreover, for several tissues it adequately predicts drug levels at two different doses, at least at the lower dose.

The present model can be improved to get a close agreement with experimental observation. The model does not precisely describe, at the two doses, the relatively narrow peak or its exact height in the brain tissue. The introduction into the model of a simple reversible mass transfer process through the brain–blood barrier accounts for the relatively slow drug entry into the brain but also results in slow drug release during the elimination phase. The observed rapid phenobarbital concentration decrease in the brain may be explained and modeled by some more

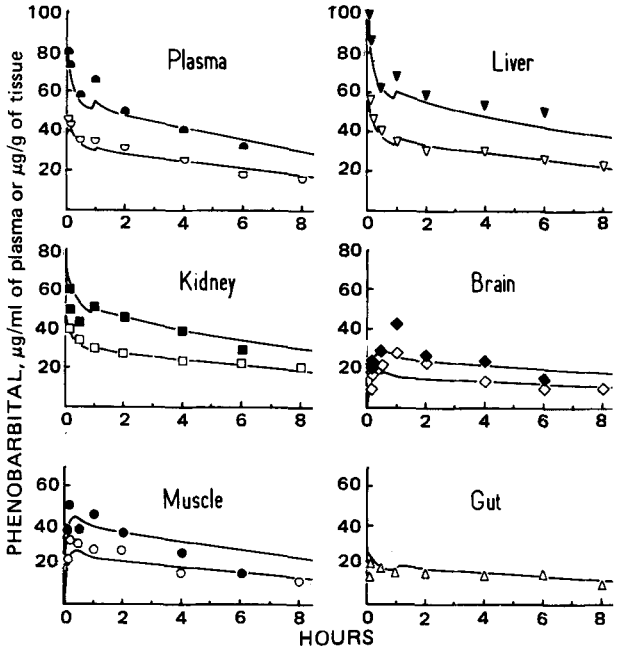

Figure 4—*Calculated time distribution of phenobarbital in various rat tissues, using the physiologically based pharmacokinetic model at 50 and 30 mg/kg. The corresponding experimental points are taken from Fig. 1. Key: solid symbols, 50 mg/kg; and open symbols, 30 mg/kg.*

complex asymmetric transport process, which greatly favors drug transport, at least during the elimination phase. Some active drug secretion from brain tissue to the peripheral blood was experimentally demonstrated for triamterene (24) and salicylic acid (25).

Another observation concerns the enterohepatic cycle, which was introduced in the model to explain the phenobarbital concentration rebound. Similar rebounds were observed in rats with morphine (27), phenolphthalein (28), and phenytoin metabolites (29). The lag time ranged from 4 to 6 hr, accounting, in addition to hepatic formation and biliary excretion, for the intestinal hydrolysis of the glucurono conjugate prior to reabsorption of the compound; this rebound did not occur with bile duct-cannulated rats (28, 29).

As demonstrated by the present model, despite continuous bile flow in the rat, phenobarbital biliary excretion followed by intestinal reabsorption can partly account for the concentration rebound observed at the higher dose ~1 hr after drug injection. This phenomenon can be theoretically obtained by considering a mean residence time of ~55 min of the drug through bile and intestine before reabsorption, provided the excreted drug concentration is sufficiently high. Autoradiographic studies with [^{14}C]phenobarbital[7] demonstrated an intensive enterohepatic recycling. On the other hand, Caldwell *et al.*[6] found that ~35% of an intraperitoneal [^{14}C]phenobarbital dose was excreted by the bile while only 1% was recovered in the feces during the first 24 hr. Moreover, unmetabolized phenobarbital seems to represent about one-third of the total gut content radioactivity. Personal experiments and other work (26) on bile duct-cannulated rats confirm the biliary excretion of unmodified phenobarbital.

However, according to this model based on a simple delay time through the enterohepatic cycle, an approximate 10-fold greater amount of phenobarbital than that experimentally observed has to be excreted in the bile to account for the observed peak height. Thus, further experiments are necessary to quantify the mechanism of biliary excretion. Moreover, if enterohepatic cycling is the actual phenomenon responsible for the concentration rebound, a more detailed representation of the cycle may be needed to improve model validity.

According to Fig. 4, phenobarbital elimination at the high dose is slightly faster than that predicted by simple first-order renal excretion and liver metabolism. A better quantitative understanding of the various elimination processes represents another prerequisite for better physiological modeling.

In the present model, a remaining distribution volume was introduced to represent all nonspecified organs and tissues. This distribution volume can account for the approximate 30% of the dose that distributes elsewhere than in blood, liver, brain, muscle, gut, and kidneys. According to autoradiographic results[7] for phenobarbital, the remaining distribution volume corresponds primarily to fat, lungs, and the heart, providing that in all tissues, except for the intestine and gut contents, there are no metabolites but only unchanged drug[6].

In conclusion, a relatively simple model based on the animal physiology and physicochemical drug parameters to a first approximation describes the main characteristics of phenobarbital pharmacokinetics. This model has many features similar to physiological models recently proposed for other compounds (3, 6, 10, 30).

[7] A. Rico, École Nationale Vétérinaire, Toulouse, France, unpublished data.

APPENDIX

b = linear binding constant (dimensionless)
C = free drug concentration (micrograms per milliliter of water)
C' = bound drug concentration (micrograms per gram of dry matter)
C^* = total drug concentration (micrograms per milliliter of blood or micrograms per gram of tissue)
D = dose (micrograms)
E = total amount eliminated by one-way metabolism, bile, or urine during a period of time (micrograms)
f = fraction of water (dimensionless)
$g(t)$ = normalized impulse injection function (minutes^{-1})
H = transport coefficient between blood and tissue (milliliters per minute)
HEM = hematocrit (dimensionless)
K = elimination constant by metabolism (K_m), bile (K_b), or urine (K_u) (milliliters per minute)
r_e = elimination rate (micrograms per minute)
r_t = drug transport rate from plasma to tissue (micrograms per minute)
t = time (minute)
T_{del} = step-delay time accounting for the biliary excretion (minute)
V = volume (milliliter)
Φ = global binding coefficient for blood or tissue (dimensionless)
θ = injection duration (minute)
Bl = blood pool
BlC = blood cells
Br = brain
G = gut
K = kidneys
L = liver
M = muscle
P = plasma
R = remaining distribution volume
T = tissue
X,Bl = blood compartment of the considered organ or tissue X
X,T = tissue compartment of the considered organ or tissue X

REFERENCES

(1) K. J. Himmelstein and R. J. Lutz, *J. Pharmacokinet. Biopharm.*, **7**, 127 (1979).

(2) H.-S. G. Chen and J. F. Gross, *Cancer Chemother. Pharmacol.* **2**, 85, (1979).

(3) L. I. Harrison and M. Gibaldi, *J. Pharm. Sci.*, **66**, 1679 (1977).

(4) K. B. Bischoff and R. L. Dedrick, *ibid.*, **57**, 1346 (1968).

(5) C. N. Chen and J. D. Andrade, *ibid.*, **65**, 717 (1976).

(6) D. B. Tuey and H. B. Matthews, *Drug Metab. Dispos.*, **5**, 444 (1977).

(7) C. Ioannides and D. V. Parke, *J. Pharm. Pharmacol.*, **27**, 739 (1975).

(8) R. Khodjett, R. Khil, A.-M. Batt, G. Siest, C. Tridon, and M. Weber, *Pathol. Biol.*, **23**, 409 (1975).

(9) F. Sarhan, J. M. Ziegler, A. Nicolas, and G. Siest, *J. Chromatogr.*, **183**, 505 (1980).

(10) C. N. Chen, D. L. Coleman, J. D. Andrade, and A. R. Temple, *J. Pharm. Sci.*, **67**, 38 (1978).

(11) T. M. Ludden, L.S. Schanker, and R. C. Lanman, *Drug Metab. Dispos.*, **4**, 8 (1976).

(12) K. B. Bischoff, R. L. Dedrick, and D. S. Zaharko, *J. Pharm. Sci.*, **59**, 149 (1970).

(13) P. L. Altman and D. S. Dittmer, "Biological Handbooks, Respiration and Circulation," Federation of American Societies for Experimental Biology, Bethesda, Maryland, 1971.
(14) A. Bonaccorsi, E. Dejana, and A. Quintana, *J. Pharmacol. Methods*, **1**, 321 (1978).
(15) I. C. Caldwell, S. Mahmood, and M. Weatherall, *J. Pharmacokinet. Biopharm.*, **6**, 521 (1978).
(16) H. H. Donaldson, "The Rat: Data and Reference Tables," 2nd ed., Wistar Institute of Anatomy and Biology, Philadelphia, Pa., 1924.
(17) D. O. Foster and M. L. Frydman, *Can. J. Physiol. Pharmacol.*, **56**, 97 (1978).
(18) A. Gjedde, J. J. Caronna, B. Hindfelt, and F. Plum, *Am. J. Physiol.*, **229**, 113 (1975).
(19) E. E. Ohnhaus and J. T. Locher, *Eur. J. Pharmacol.*, **31**, 161 (1975).
(20) Y. Sasaki and H. N. Wagner, *J. Appl. Physiol.*, **30**, 879 (1971).
(21) W. S. Spector, "Handbook of Biological Data," Saunders, Philadelphia, Pa., 1956.
(22) L. Takács, L. A. Debreckzni, and C. Farsang, *J. Appl. Physiol.*, **38**, 696 (1975).
(23) F. Vetterlein, R. Halfter, and G. Schmidt, *Arzneim-Forsch*, **29**, 747 (1979).
(24) A. W. Pruitt, J. L. McNay, and P. G. Dayton, *Drug Metab. Dispos.*, **3**, 30 (1975).
(25) M. A. Gonzalez, T. N. Tozer, and D. T. T. Chang, *J. Pharm. Sci.*, **64**, 99 (1975)
(26) D. Y. Cooper, H. Schleyer, S. S. Levin, J. C. Touchstone, R. H. Eisenhardt, H. M. Vars, O. Rosenthal, H. Rastigar, and A. Harken, in "The Introduction of Drug Metabolism," R. W. Estabrook and E. Lindenlaub, Eds., Symposia Medica Hoechst, Verlag, Stuttgart, West Germany, 1979, pp. 253–256.
(27) B. E. Dahlström and L. K. Paalzow, *J. Pharmacokinet. Biopharm.*, **6**, 505 (1978).
(28) W. A. Colburn, P. C. Hirom, R. J. Parker, and P. Milburn, *Drug Metab. Dispos.*, **7**, 100 (1979).
(29) A. M. El-Hawari and G. L. Plaa, *ibid.*, **6**, 59 (1978).
(30) M. Mintun, K. J. Himmelstein, R. L. Schroder, M. Gibaldi, and D. D. Shen, *J. Pharmacokinet. Biopharm.*, **8**, 373 (1980).

Solubility Behavior of Barbituric Acids in Aqueous Solution of Sodium Alkyl Sulfonate as a Function of Concentration and Temperature

C. VAUTION *, C. TREINER ‡ ×, F. PUISIEUX *, and J. T. CARSTENSEN §

Received January 5, 1981, from the *Laboratoire de Pharmacie Galénique, Faculté de Pharmacie, Rue Jean Baptiste Clément, 92290 Chatenay Malabry, France*, the ‡ *Laboratoire d'Electrochimie, Université Pierre et Marie Curie, 4 Place Jussieu, Bâtiment F, 75005, Paris, France*, and the § *School of Pharmacy, University of Wisconsin, Madison, WI 53706.* Accepted for publication March 25, 1981.

Abstract □ The solubility of 13 barbituric acids was determined in aqueous solutions of sodium alkyl sulfonate. The effects of concentration and temperature were investigated, and the thermodynamic functions of the solubilization process were calculated. An analysis of the location of a solubilized species within a micelle is suggested in terms of the sign and amplitude of the standard entropy of solubilization, which is strongly positive for micelle penetration and negative for adsorption. A solubilization mechanism through adsorption onto the micellar surface is suggested for most of the barbituric acids studied. The enthalpy/entropy compensation phenomenon was identical for barbituric acids in ionic and nonionic (polyoxyethylene lauryl ether) surfactant solutions with a compensation temperature of 270 °K, indicating common behavior of these compounds with respect to micellar solubilization. The concept of molecular surface area was used to correlate the free energy of solubilization of the solutes to their size and structure. A linear relationship was found with an excellent correlation factor for the alkane derivatives of the 5-ethyl-barbituric acids. The specific behavior of some of the barbituric acids investigated is discussed.

Keyphrases □ Solubility—barbituric acids in aqueous sodium alkyl sulfonate, thermodynamics □ Thermodynamics—solubility of barbituric acids in aqueous sodium alkyl sulfonate □ Barbituric acids—solubility in aqueous sodium alkyl sulfonate, thermodynamics

The increase in solubility of poorly soluble preservatives in water by the addition of surfactants has been the subject of a large number of studies (1, 2). This phenomenon is related to the formation of micelles in water, but the availability of the preservative as an active agent is highly dependent on the molecular attachment site, and this subject is still a controversial matter. Opposite views have been proposed for barbituric acids, such as adsorption at the micelle interface (3) or incorporation into the micelle hydrocarbon core (4). However, for simpler molecules like acetone or urea, which may be considered model compounds for barbituric acids, thermodynamic evidence shows that these molecules hardly penetrate the micelle interior, at least at the critical micelle concentration (CMC) and for ionic micelles (5, 6).

BACKGROUND

Studies on the solubilization of barbituric acids have been mostly (7) restricted to the influence of nonionic surfactants (3, 4, 8–10). Few of these studies were concerned with the determination of thermodynamic functions such as free energy, enthalpy, and entropy (3). In fact, few papers have been published on this subject for compounds other than barbituric acids (3, 11, 12).

The present work investigated the solubilization properties of sodium alkyl sulfonate. Its biodegradability and nontoxic properties, even at high surfactant concentration, make it an interesting surfactant in formulation problems (13). The barbituric acids are useful compounds in this respect since the possibility of changing, almost at will, the radicals attached to the malonylurea ring permits the study of the influence of shape and structure on the solubilization process. Thus, previous studies (14) on the molecular surface area concept and the investigation of the effects of temperature on barbituric solutions have indicated the use of the entropy function to deduce the chemical environment of compounds solubilized by micelles.

EXPERIMENTAL

Materials—Sodium alkyl sulfonate[1] was composed of 90.7% (by weight) monosulfonated detergent, 8.8% polysulfonated compound, and 0.5% unsulfonated product. The monosulfonated compound was a mixture of $C_{14}H_{29}SO_3Na$ and $C_{15}H_{31}SO_3Na$, so a molecular weight of 323 was adopted in the concentration calculations. The CMC of the detergent

[1] Produits chimiques de la Montagne Noire, 81100, Castres, France.

0022-3549/81/1100-1238$01.00/0